

1 **Supplementary material (SI)**

2  
3  
4 **Evaluating pesticide degradation in artificial wetlands with compound-specific**  
5 **isotope analysis: a case study with the fungicide dimethomorph**  
6

7 *Tetyana Gilevska<sup>1</sup>, Sylvain Payraudeau<sup>1</sup>, Gwenaël Imfeld<sup>1</sup>*

8 <sup>1</sup> Université de Strasbourg, CNRS/ENGEEES, ITES UMR 7063, Institut Terre et Environnement de  
9 Strasbourg, Strasbourg, France

10  
11 **S1. Chemicals**

12 Solvents (dichloromethane (DCM), acetonitrile (ACN), ethyl acetate (EtOAc), and methanol  
13 (MeOH)) were HPLC grade purity (>99.9%) and purchased from Sigma–Aldrich. Analytical  
14 standards (purity >98%) of atrazine, metalaxyl, *S*-metolachlor, *S*-metolachlor D-11, cyprodinil,  
15 pyrimethanil, terbuthylazine, pendimethalin, terbuthylazine, tebuconazole, and DIM (Z and E  
16 isomers) were purchased from Sigma–Aldrich, PESTANAL. Pesticide stock solutions were  
17 prepared in ACN at 1 g/L and stored at -18 °C. An intermediate solution in DI water for spiking  
18 during laboratory experiments was prepared according to pesticide solubilities. Chemical  
19 integrative samplers (POCIS) were assembled as described previously (Gilevska et al., 2022).

## 21 **S2. DIM degradation half-lives**

22 Pseudo first-order kinetics were assumed for all degradation experiments. An exponential curve  
23 was fitted with the concentration ( $c$ ) at the time ( $t$ ), the initial concentration ( $c_0$ ), and the pseudo-  
24 first-order rate constant  $k$ :

$$25 \quad c = c_0 \times \exp(-k \times t) \quad \text{Equation S1}$$

26 The half-life (days) was determined as:

$$27 \quad t_{1/2} = \frac{\ln 2}{k} \quad \text{Equation S2}$$

28 Uncertainty was derived from the regression analysis in equation S1.

## 29 **S3. Quantification of pesticides by GC-MS**

30 Quantitative analysis was carried out by gas chromatography (GC, Trace 1300, Thermo  
31 Fisher Scientific) coupled with a mass spectrometer (MS, ISQ™, Thermo Fisher Scientific).  
32 Metolachlor-d<sub>11</sub> was automatically added in each sample as an internal standard at a constant  
33 concentration by the autosampler (TriPlus RSH™, Thermo Fisher Scientific). S-metolachlor D-11  
34 was injected with every injection to account for the reproducibility of the autosampler. The samples  
35 (1 μL volume) and internal standard (1 μL at 300 μg/L) were injected into a split/splitless injector  
36 operated in split mode with a split flow at 6.0 mL/min and held at 280 °C. Separation was  
37 performed on a TG-5MS column (30 m × 0.25 mm ID, 0.25 μm film thickness), with helium as  
38 carrier gas at a 1.5 mL/min flow rate. The GC oven program was held at 50 °C for 1 min, ramped  
39 to 160 °C at 30 °C/min, then to 220 °C at 4 °C/min, and finally to 300 °C at 30 °C/min held for 1  
40 min. The MS transfer line and source were heated at 320 °C. The best sensitivity in the multiple  
41 reaction monitoring operation (MRM) mode was achieved through the acquisition of selected  
42 reaction monitoring (SRM) transitions. For compound identification, two SRM transitions and a

43 correct ratio between the abundances of two optimized SRM transitions (SRM1/SRM2) were  
44 required along with retention time matching. Each sample was measured in triplicate. Detection  
45 limits (DLs) were 5 to 8 µg/L and quantification limits (QLs) were 17 to 23 µg/L depending on the  
46 compound.

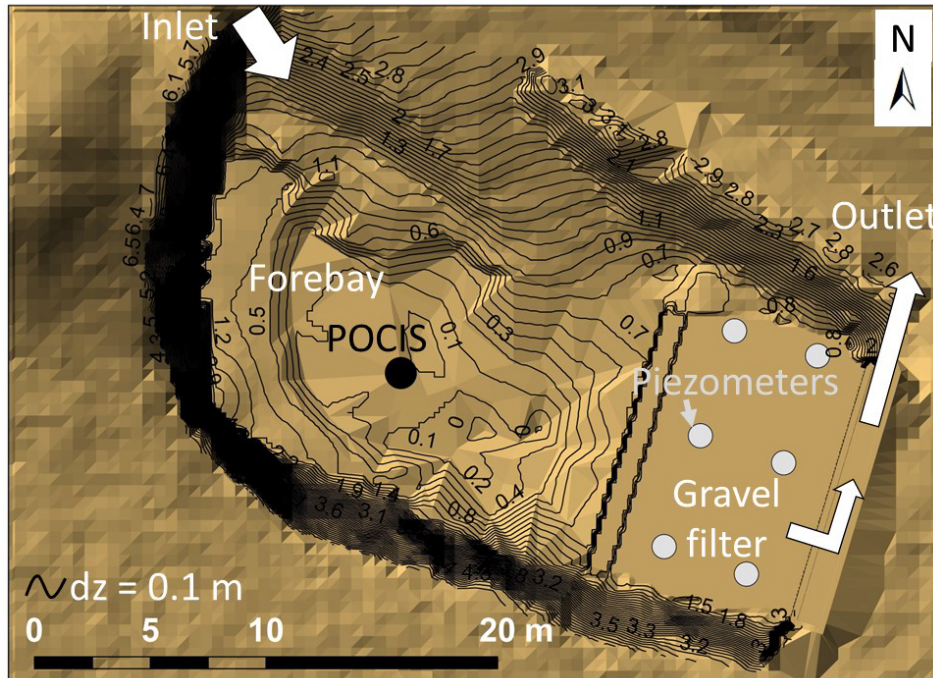
47 Changes in the E/Z ratios of DIM were calculated with isomer fractionation  $IF(Z)$  (Masbou  
48 et al., 2022), according to equation S3:

$$49 \quad IF(Z) = \frac{DIM\ Z}{(DIM\ Z + DIM\ E)} \quad \text{Equation S3}$$

50

#### 51 **S4. Hydrological model**

52 The model considered the water discharge at the wetland inlet from the upstream catchment,  
53 the direct rainfall (Meteorological station, Meteo France, station n°68287003 located in the  
54 upstream catchment, 6-minutes time step), the evapotranspiration and the outflow. Due to the  
55 clayed wetland bed (permeability  $<10^{-10}$  m/s) limiting water infiltration towards groundwater, and  
56 based on previous water mass balance (Imfeld et al., 2013), the water loss by vertical infiltration  
57 was assumed negligible. The outflow discharges were estimated with the Toricelli formula using  
58 the section and elevation of the outflow pipes and the elevation-storage function of the wetland  
59 (Figure S1)

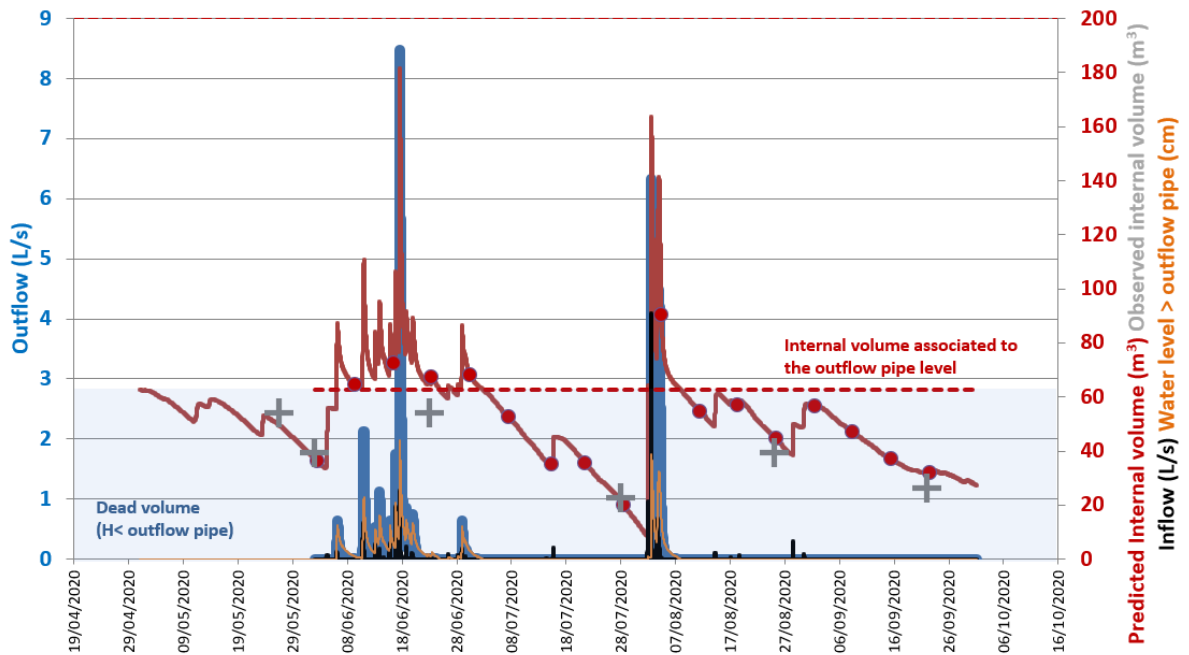


60

61 Figure S1. Artificial wetland topography from upstream to downstream forebay with the POCIS,  
 62 and the gravel filter with six piezometers

63

64 The elevation of the different outflow pipes was measured (considering  $z = 0$  for the deepest point  
 65 of the wetland) and the elevation-storage function of the wetland were derived from airborne  
 66 LiDAR combined with additional terrestrial topographic measurements. The daily  
 67 evapotranspiration of the wetland was calibrated according to the Penman–Monteith potential  
 68 evapotranspiration (from the meteorological station) to minimize the difference between the  
 69 predicted and the observed water levels in the wetland over the study period. The comparison  
 70 between predicted and observed water elevation within the wetland was  $<3.5 \pm 1.5$  cm ( $n = 6$ )  
 71 (Figure S2)



72  
 73 Figure S2: Hydrological dynamic with the observed inflow (dark grey), the predicted and observed  
 74 internal volume (grey cross and dark brown, respectively), and predicted water level > outflow  
 75 pipe used in the Torricelli formula to calculate wetland outflow (orange), with 6 pictures describing  
 76 the water storage in the wetland forebay from June 2<sup>nd</sup> to August 11<sup>th</sup>

77 The uncertainty associated with elevations was propagated in the elevation-storage function and  
 78 the water volume of the wetland compartments.

79

80 **S5. AKIE calculation**

81 The apparent kinetic isotope effect (AKIE) was calculated according to (Elsner, 2010):

82  $AKIE = 1 / (1 + z * \epsilon_{\text{reactive position}} / 1000)$  Equation S4

83 where ( $z$ ) is the number of atoms that are in intramolecular competition and  $\epsilon_{\text{reactive position}}$  is the  
84 isotopic fractionation value in the reactive position, which is calculated from the following  
85 equation:

$$86 \quad \epsilon_{\text{reactive position}} \approx n/x * \epsilon \quad \text{Equation S5}$$

87 where ( $n$ ) is the total number of atoms, ( $x$ ) is the number of atoms that would experience isotope  
88 effects in the given mechanistic scenario, and ( $\epsilon$ ) is the bulk isotope fractionation value of the  
89 reaction. In the case of DIM anoxic degradation:  $n=21$ ,  $x=z=1$ .

90

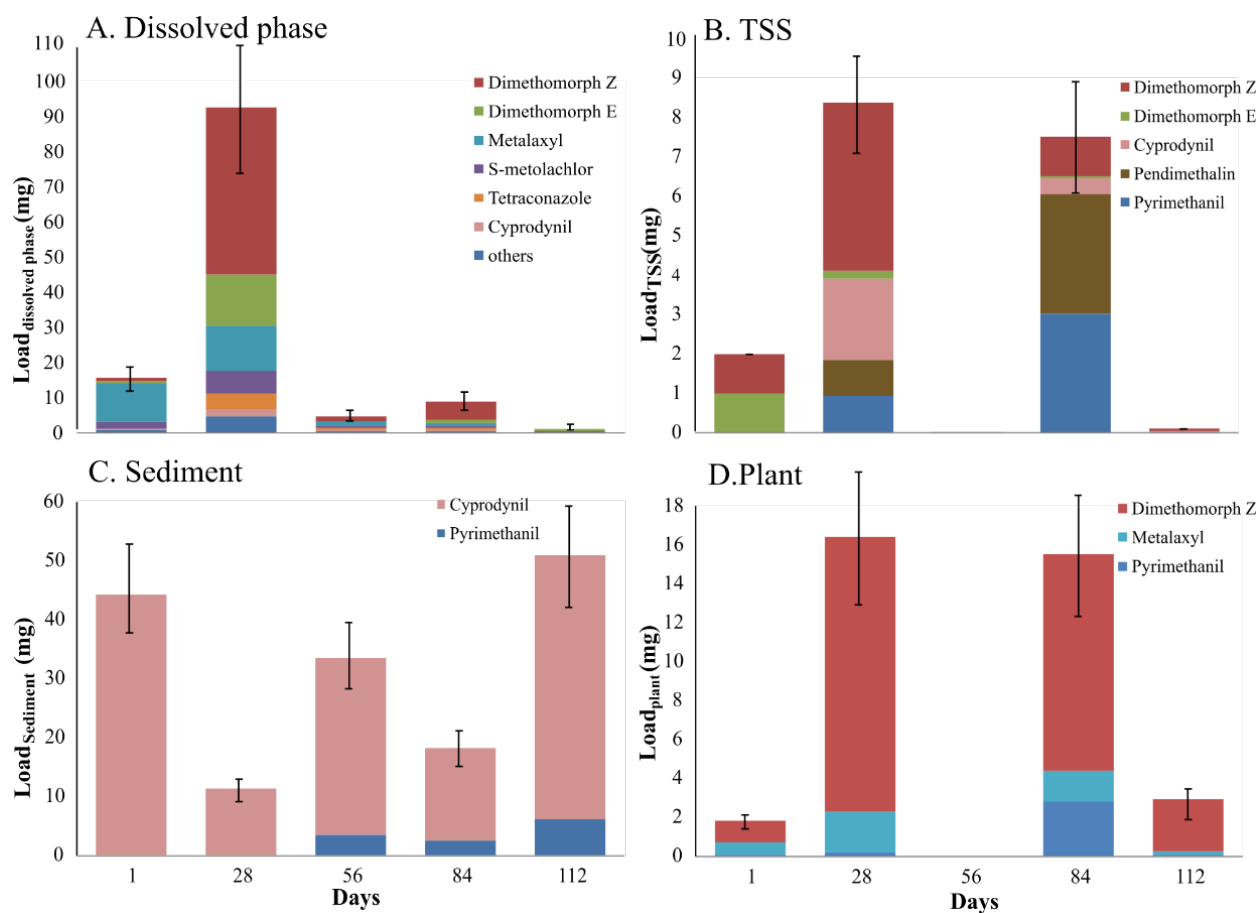
## 91 **S6. Pesticide distribution among wetland compartments**

92 Over the period of the sampling campaign, six fungicides (dimethomorph (DIM),  
93 cyprodinil, metalaxyl, pyrimethanil, tebuconazole, tetraconazole) and four herbicides  
94 (pendimethalin, S-metolachlor, atrazine, terbuthylazine) were detected in the stormwater wetland.  
95 Most pesticides were applied in June, resulting in high pesticide input from run-off (first "wet"  
96 period, 1422 + 205 mg) (Table S4). Overall, the highest load and number of detected pesticides  
97 can be found in dissolved phases with wet periods having much higher loads than dry periods  
98 (Table S4).

99 Worthy of note, DIM, cyprodinil, metalaxyl, pyrimethanil, terbuthylazine, and  
100 tetraconazole were also detected in the Rouffach stormwater wetland in 2003-2006, 2009, and 2011  
101 (Grégoire et al., 2010; Maillard and Imfeld, 2014; Maillard et al., 2011). Despite some interannual  
102 variations of both hydroclimatic conditions and used pesticides, pesticide concentrations and  
103 loadings in runoff entering the wetland have decreased by 4-fold in two decades. This indicates  
104 that the gradual conversion of up to 50% of vineyard plots of the catchment to organic farming

105 practices drastically reduced pesticide exports, although pesticide residues and transformation  
 106 products may still be mobilized from recently converted organic farming plots (Riedo et al., 2021).

107 Partitioning of pesticides between water, TSS, sediments, and plants could be related to the  
 108 physicochemical properties of pesticides. Pesticides with  $\text{LogKow} > 3$  were detected mainly in TSS,  
 109 sediment, and plants, e.g., cyprodinil (Figure S3, Table S4). Nevertheless, metalaxyl ( $\text{LogKow} =$   
 110 1.8, solubility = 8.4 g/L) was detected in the aerial part of the *Phragmites australis*, confirming its  
 111 translocation potential (Gong et al., 2020).



112  
 113 Figure S3. Pesticide distribution among the wetland compartments: (A) Dissolved phase, (B) TSS-  
 114 total suspended solids, (C) Sediment, (D) Plants. Day 1 (June 2<sup>nd</sup>), 28 (June 30<sup>th</sup>), 56 (July 28<sup>th</sup>),  
 115 84 (August 30<sup>th</sup>), and 112 (September 22<sup>nd</sup>) across the study period. The error given for the

116 pesticide loads was calculated via error propagation through the hydrological model (see section  
117 2.6.4, main text).

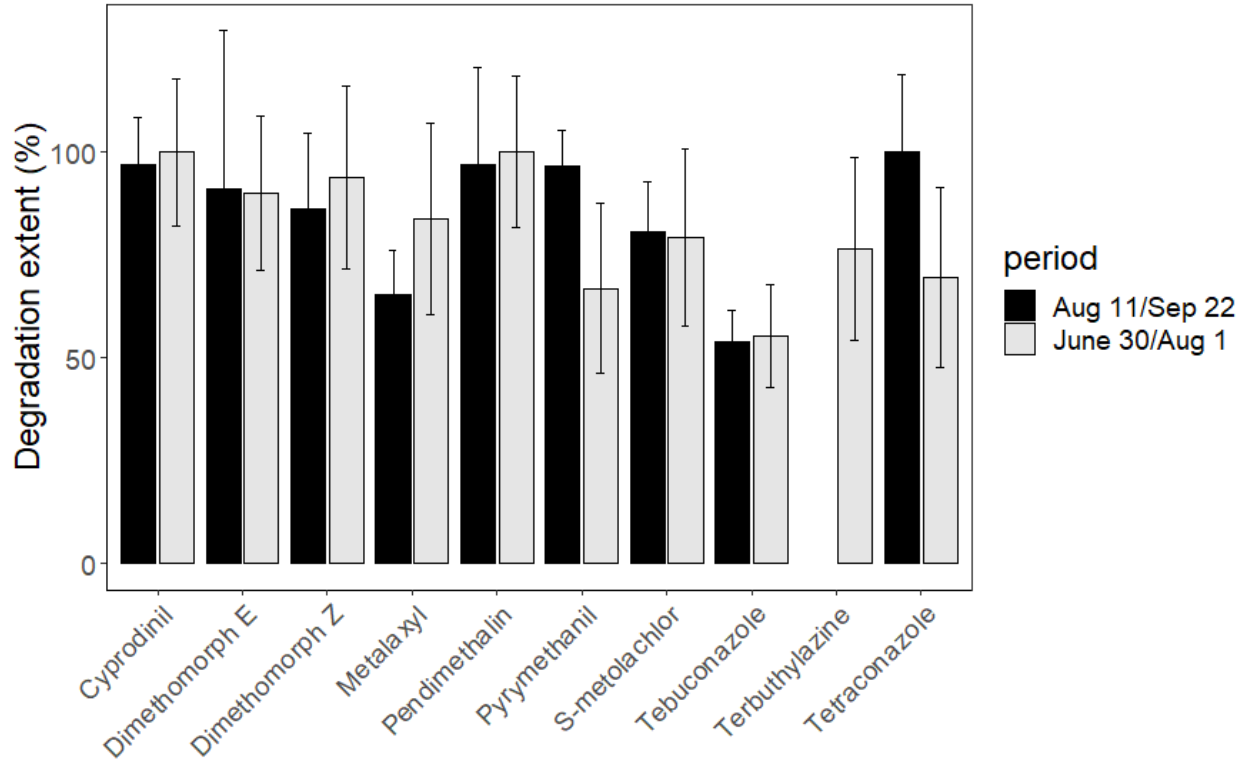
118

### 119 **S7. Pesticide degradation in the wetland based on concentrations and mass balance.**

120 Pesticide degradation in wetland based on concentration data (Equation 5, main text) was  
121 estimated when outflow was not active in the wetland, i.e., during July and after August 11<sup>th</sup> until  
122 September 22<sup>nd</sup>. Pesticide degradation calculated this way ranged from 65 to 100% for the 10  
123 pesticides during the dry periods (Figure S4). Since atrazine was detected only in June, atrazine  
124 dissipation could not be estimated in this study. Similar dissipation rates were obtained for DIM,  
125 cyprodinil, metalaxyl, pyrimethanil, terbuthylazine, and tetraconazole in the same stormwater  
126 wetland in 2009 and 2011 (Maillard and Imfeld, 2014; Maillard et al., 2011). Hence, the sediment  
127 removal in early 2020 did not affect pesticide dissipation and the removal efficiency of the  
128 stormwater wetland did not vary much over a decade.

129





130

131 Figure S4. Degradation of pesticide loads in the stormwater wetland during the dry periods. The  
 132 error given for the pesticide loads was calculated via error propagation of the hydrological model  
 133 (see section 2.6.4).

134 Table S1. Hydrochemistry of the wetland over the period of sampling campaigns. Analytical  
 135 uncertainties were 5% for major ions, metals, and carbon concentrations. Precision was  $\pm 0.5\%$  for  
 136 conductivity, and  $\pm 0.01$  unit for pH. TOC: total organic carbon, DOC: dissolved organic carbon,  
 137 TSS: total suspended solids, E.C: electrical conductivity. \* - means total iron, nd. - means not  
 138 detected (below detection limit).

	Unit	Wet period/June 2 <sup>nd</sup> - June 30 <sup>th</sup>	Dry period/June 30 <sup>th</sup> - August 1 <sup>st</sup>	Wet period/August 1 <sup>st</sup> - August 11 <sup>th</sup>	Dry period/August 11 <sup>th</sup> - September 22 <sup>nd</sup>
pH	-	7,0 $\pm$ 0,5	6,8 $\pm$ 0,6	7,2 $\pm$ 0,5	7,3 $\pm$ 0,6
E.C.	$\mu$ S/cm	500 $\pm$ 25	535 $\pm$ 14	560 $\pm$ 60	490 $\pm$ 55
Temp	$^{\circ}$ C	11.9 -27.0	22,4 $\pm$ 3,5	20,1 $\pm$ 4,5	17,2 $\pm$ 2,5
TOC	mg/L	11,6 $\pm$ 2,3	10,6 $\pm$ 3,0	9,0 $\pm$ 2,3	10,5 $\pm$ 2,0
DOC	mg/L	10,3 $\pm$ 1,0	10,2 $\pm$ 2,2	8,0 $\pm$ 1,0	10,0 $\pm$ 1,0
TSS	mg/L	40 $\pm$ 26	69 $\pm$ 52	32 $\pm$ 10	42,3 $\pm$ 19
Na <sup>+</sup>	mg/L	6,0 $\pm$ 1,8	9,8 $\pm$ 2,2	4,1 $\pm$ 1,1	10,7 $\pm$ 4,3
Mg <sup>2+</sup>	mg/L	7,0 $\pm$ 1,7	10,2 $\pm$ 1,6	5,2 $\pm$ 1,9	9,4 $\pm$ 1,9
K <sup>+</sup>	mg/L	5,2 $\pm$ 0,5	4,7 $\pm$ 0,5	5,8 $\pm$ 1,2	4,0 $\pm$ 1,0
Fe <sup>3+</sup>	mg/L	0.2 - 1	0,8 - 2,2	1 - 2,0	1,5 - 2,8
Fe <sup>2+</sup>	mg/L	0.8 - 1,2	1 - 1,8	1,5 - 2,2	2 - 3,3
SO <sub>4</sub> <sup>2-</sup>	mg/L	23,5 $\pm$ 11,4	17,6 $\pm$ 4,6	40,1 $\pm$ 8,4	29,1 $\pm$ 7,2
NO <sub>2</sub> <sup>-</sup>	mg/L	nd - 0,6	nd - 0,4	nd - 0,5	nd - 2.7
NO <sub>3</sub> <sup>-</sup>	mg/L	0,2 $\pm$ 0,0	nd	nd	2,6 $\pm$ 00
NH <sub>4</sub> <sup>+</sup>	mg/L	0,2 $\pm$ 0,2	0,1 $\pm$ 0,0	nd	1,9 $\pm$ 1,3
Cl <sup>-</sup>	mg/L	11,1 $\pm$ 3,7	19,1 $\pm$ 4,3	7,4 $\pm$ 0,14	15,2 $\pm$ 5,0

139

140

141

142

143

144

145 Table S2. Sediment properties. Analytical uncertainty is 5% for the major elements.

Parameter	Fraction	Date			
		02/06/2020	28/07/2020	22/09/2020	02/12/2020
% Clay	> 2 $\mu$ m	20.8	23.2	21.2	25.9
% Silt	2 $\mu$ m - 50 $\mu$ m	60.7	60.2	62.2	57.6
% Sand	50 $\mu$ m - 2000 $\mu$ m	18.5	16.6	16.6	16.5
% Carbonate	< 2 mm	23.3	23.7	25.4	22.7
% TOC	< 100 $\mu$ m	5.6	5.4	5.8	4.6
% Total N	< 100 $\mu$ m	0.3	0.3	0.3	0.2
% DOC	< 2 mm	2.8	2.6	2.7	1.9
pH	< 2 mm	7.5	7.6	7.6	7.6
SiO <sub>2</sub>	< 2 mm	49.0	47.9	48.7	49.8
Al <sub>2</sub> O <sub>3</sub>	< 2 mm	9.98	9.61	9.90	10.9
MgO	< 2 mm	1.85	1.74	1.84	2.02
CaO	< 2 mm	13.3	14.2	13.4	12.7
Fe <sub>2</sub> O <sub>3</sub>	< 2 mm	4.24	4.08	4.17	4.46
MnO	< 2 mm	0.074	0.073	0.074	0.087
TiO <sub>2</sub>	< 2 mm	0.550	0.527	0.548	0.582
Na <sub>2</sub> O	< 2 mm	0.64	0.65	0.60	0.52
K <sub>2</sub> O	< 2 mm	2.21	2.10	2.16	2.32
P <sub>2</sub> O <sub>5</sub>	< 2 mm	0.294	0.319	0.293	0.243

146

147

148

149

150

151

152

153

154 Table S3. Calculation of pesticide mass in each compartment

Wetland compartment	Samples	Pesticide mass (M)	Units
Dissolved phase	Inlet, grab	$C_{\text{pest diss}} \times V_{\text{water compartment}}$	$\text{mg}=(\text{ng/L}/1000/1000) \times (\text{L} \times 1000)$
TSS	Inlet, grab, piezo	$C_{\text{pestTSS}} \times C_{\text{TSS}} \times V_{\text{water compartment}}$	$\text{mg}=(\text{mg/kg}) \times (\text{L} \times 1000) \times (\text{mg/L}/1000)$
Phragmites roots/Cattail/Lemna	Whole area	$C_{\text{pestPhr}} \times M_{\text{Phr of 1 plant}} \times \text{Density}_{\text{Phr}} \times \text{Area}_{\text{wetland}} \times \text{Coverage}$ $C_{\text{pestLemna}} \times M_{\text{Lemna on m}^2} \times \text{Area}_{\text{wetland}} \times \text{Coverage}$	$\text{mg}=(\mu\text{g/kg}/1000) \times (\text{g}/\text{stem}/1000) \times (\text{stem}/\text{m}^2) \times \text{m}^2 \times (\%/100)$ $\text{mg}=(\mu\text{g/kg}/1000) \times (\text{kg}/\text{m}^2) \times \text{m}^2 \times (\%/100)$
Sediment	Forebay	$C_{\text{pest SED}} \times \text{Density}_{\text{sediment}} \times \text{Volume}$	$\text{mg}=(\text{mg/kg}/1000) \times (\text{kg}/\text{m}^3) \times (\text{m}^3)$

155 *Assumptions for concentration mass balance: Phragmatis: Weight of one Phragmatis - 1.6 g dry weight ((Min, 2015)mass of 1*  
 156 *plant), density taken from the (Maillard and Imfeld, 2014), coverage calculated based on photos; Lemna minor: Weight 1.2 kg wet*  
 157 *weight/m<sup>2</sup> - 0.12 kg dry weight/m<sup>2</sup>, coverage calculated based of photos.; Sediment: Volume 234m<sup>2</sup>\*10cm*  
 158 *Assumptions for isotope mass balance: several inlets (June 30<sup>th</sup>, and August 4<sup>th</sup>, 25<sup>th</sup>) carbon isotopic signatures of DIM Z were*  
 159 *assumed based on the previous and/or next week's carbon isotope signature of the DIM Z. On September 22<sup>nd</sup> grab isotopic*  
 160 *signature was below the detection limit for carbon CSIA of DIM Z, therefore POCIS isotopic signature (sampled on the 22<sup>nd</sup> of*  
 161 *September) was used instead.*

162  
 163  
 164

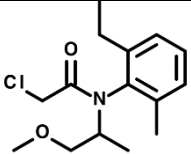
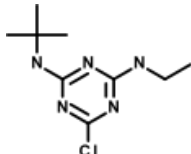
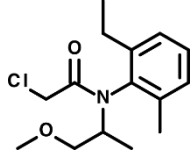
165 Table S4. Total pesticide loads (mg) in runoff water entering the stormwater wetland (inlet) in the dissolved  
 166 phase and in total suspended solids (TSS), - means below detection limit.

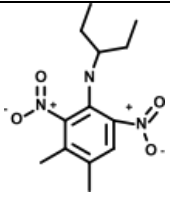
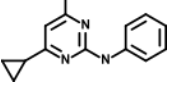
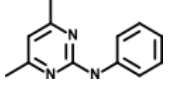
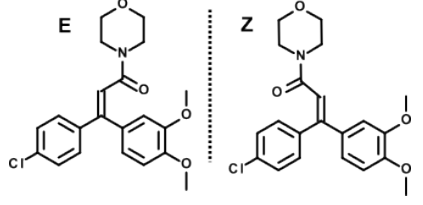
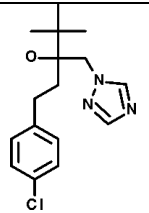
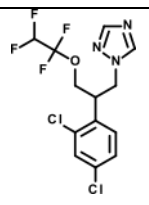
167

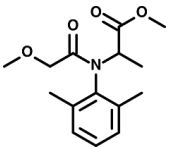
Compound	Wet period/June 2 <sup>nd</sup> - June 30 <sup>th</sup>	Dry period/June 30 <sup>th</sup> – August 1 <sup>st</sup>	Wet period/August 1 <sup>st</sup> – August 11 <sup>th</sup>	Dry period/August 11 <sup>th</sup> – September 22 <sup>nd</sup>
Compound	Total pesticide loads inlet (mg)_ dissolved phase			
DIM Z	845.9 ± 157.9	2.0 ± 0.4	96.2 ± 15.6	7.3 ± 1.7
DIM E	253.3 ± 0.1	0.7 ± 0.1	36.7 ± 6.0	2.5 ± 0.6
Cyprodinil	21.9 ± 4.1	0.1 ± 0.0	5.0 ± 0.8	0.2 ± 0.2
Metalaxyl	45.0 ± 6.7	0.9 ± 0.1	39.8 ± 6.0	2.0 ± 0.3
S-metolachlor	54.9 ± 8.2	0.7 ± 0.1	30.8 ± 4.6	1.5 ± 0.2
Tetraconazole	28.8 ± 4.3	0.1 ± 0.0	5.2 ± 0.8	0.3 ± 0.1
Terbuthylazine	18.7 ± 2.8	0.0 ± 0.0	-	-
Pendimethalin	0.8 ± 0.1	0.1 ± 0.0	6.1 ± 1.0	0.2 ± 0.2
Tebuconazole	49.9 ± 7.5	0.1 ± 0.0	3.3 ± 0.5	0.1 ± 0.0
Pyrimethanil	4.6 ± 0.9	0.1 ± 0.0	3.6 ± 0.6	0.2 ± 0.0
Atrazine	5.3 ± 0.8	-	-	-
Total	1329.1 ± 193.4	4.7 ± 0.7	226.7 ± 35.9	14.3 ± 3.3
Compound	Total pesticide loads inlet (mg)_ TSS			
DIM Z	45.0 ± 8.6	0.9 ± 0.2	40.0 ± 6.5	3.4 ± 0.8
DIM E	0.9 ± 0.2	0.1 ± 0.0	0.0 ± 0.0	0.9 ± 0.2
Cyprodinil	32.1 ± 0.0	0.9 ± 0.0	24.5 ± 2.6	1.3 ± 0.3
Metalaxyl	-	-	-	-
S-metolachlor	-	-	-	-
Tetraconazole	-	-	-	-
Terbuthylazine	-	-	-	-
Pendimethalin	18.0 ± 3.5	0.2 ± 0.0	15.1 ± 2.4	1.1 ± 0.25
Tebuconazole	-	-	-	-
Pyrimethanil	0.2 ± 0.0	0.1 ± 0.0	13.0 ± 0.8	0.7 ± 0.2
Atrazine	-	-	-	-
Total	96.3 ± 13.2	3.1 ± 1.4	92.6 ± 12.0	7.9 ± 2,5

168 Table S5. Chemical physico-chemical characteristics of the studied compounds. NA – not applicable, - not measured. (1) -

169 <http://sitem.herts.ac.uk/aeru/>

Common name	Use	Approval in EU (revision date) (1)	Structure	Chemical family	Chemical formula	Half-life in Water-sediment (days) (1)	Solubility in water (20 °C, mg L <sup>-1</sup> ) (1)	Octanol/water coefficient (LogK <sub>ow</sub> ); pH7, 20°C)	pK <sub>a</sub> , 25°C	Sorption capacities, logK <sub>oc</sub>	
										Experimental Rouffach sediment (Droz et al., 2021)	Predicted consensus from EPA CompTox (Williams et al., 2017)
atrazine	herbicides	banned (2004)		Triazine	C <sub>8</sub> H <sub>14</sub> ClN <sub>5</sub>	80	35	2.7	1.7	1.5 – 2.6	2.1 – 2.2
terbuthylazine		approved (2024)			C <sub>9</sub> H <sub>16</sub> ClN <sub>5</sub>	70	6.6	3.4	1.9	-	2.3
S-metolachlor		approved (2019)		Acetanilide	C <sub>15</sub> H <sub>22</sub> ClNO <sub>2</sub>	47	480	3	NA	2.3 – 2.6	2.4 – 2.5

pendimethalin	approved (2024)		Dinitroaniline	$C_{13}H_{19}N_3O_4$	16	0.33	5.4	2.8	-	3.7 – 4.2
cyprodinil	approved (2023)		Anilinopyrimidine	$C_{12}H_{15}N_3$	142	13	4	4.4	-	3.3 – 3.5
pyrimethanil	approved (2023)		Anilinopyrimidine	$C_{12}H_{13}N_3$	81	110	2.8	3.5	-	2.9
dimethomorph (DIM)	approved (2022)		Morpholine	$C_{21}H_{22}ClNO_4$	38	29	2.7	-1.3	-	2.4 – 3.4
tebuconazole	approved (2022)		Triazole	$C_{16}H_{22}ClN_3O$	365	36	3.7	5.0	-	2.6 – 3.0
tetraconazole	approved (2022)		Triazole	$C_{13}H_{11}Cl_2F_4N_3$	340	156	3.6	0.65	-	2.8

metalaxyl		approved (2023)		Phenylamide	$C_{15}H_{21}NO_4$	32	8400	1.8	1.4 [3]	1.1 – 1.7	1.6 – 1.7
-----------	--	--------------------	---	-------------	--------------------	----	------	-----	------------	-----------	-----------

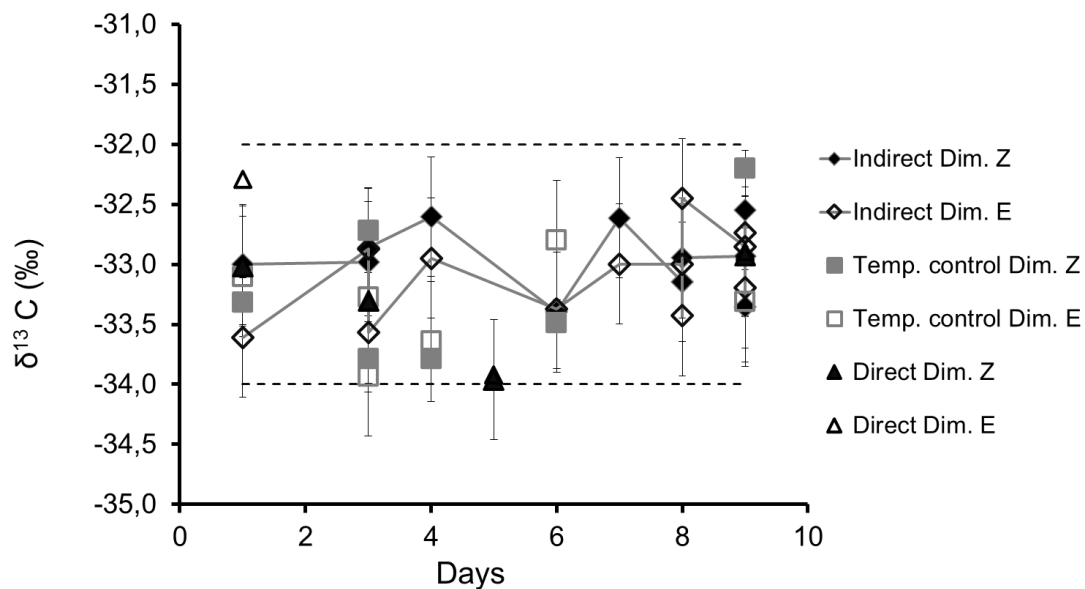
170

171



172

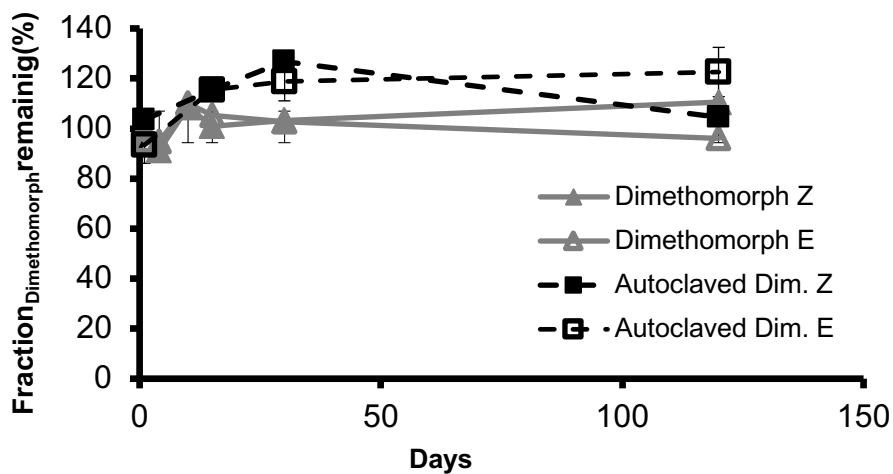
173



174

175 Figure S5. Carbon stable isotope signature ( $\delta^{13}\text{C}$ ) for Z (filled symbols) and E (empty symbols) isomers  
176 of DIM under indirect photolysis (diamond), direct photolysis (triangles), and control (squares). Dashed  
177 lines represent  $\pm 1\%$  from the  $\delta^{13}\text{C}$  standard value.

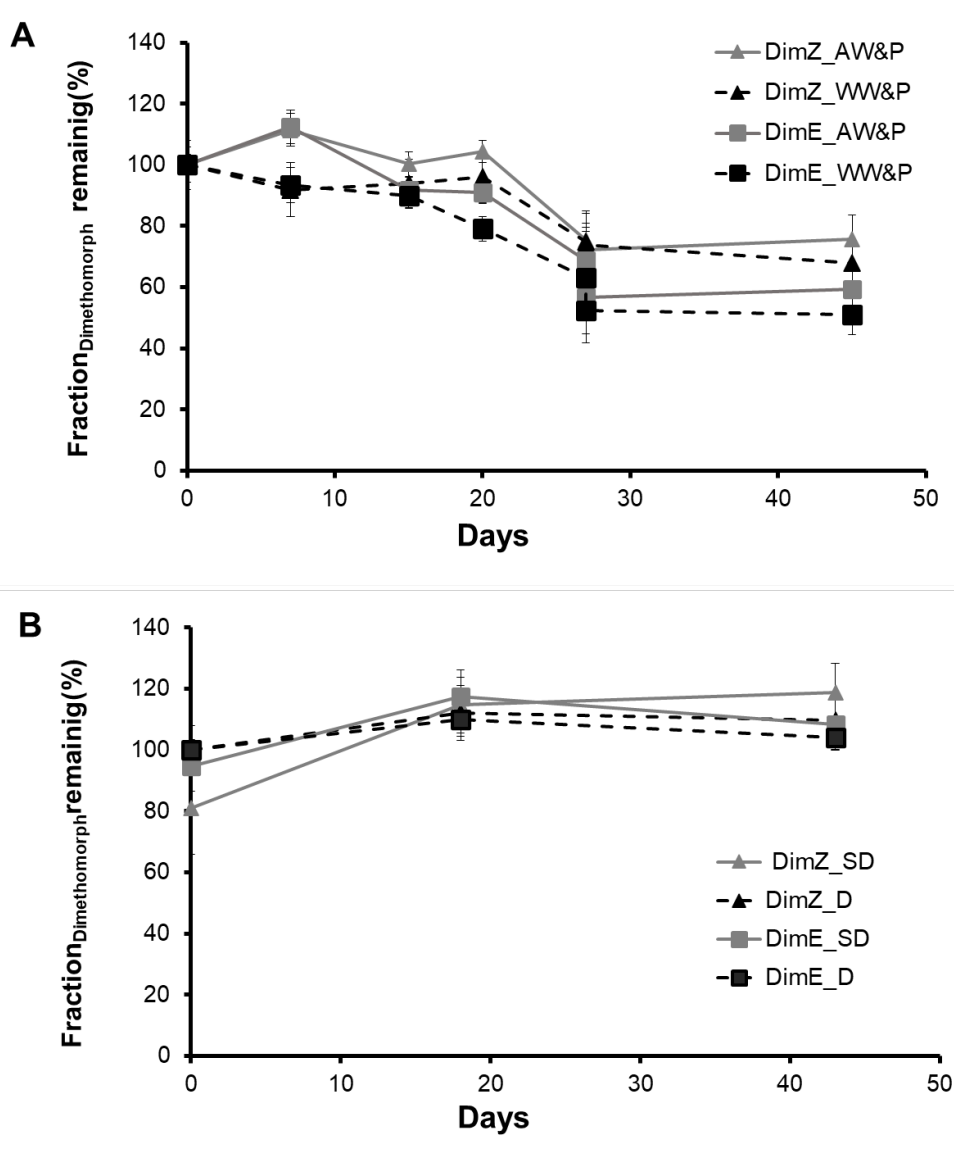
178



179

180 Figure S6. Fraction remaining of Z (triangles) and E (squares) isomers of DIM over time during  
181 oxic biodegradation with wetland water experiment with autoclaved (empty symbols) and live  
182 microcosms (filled symbols).

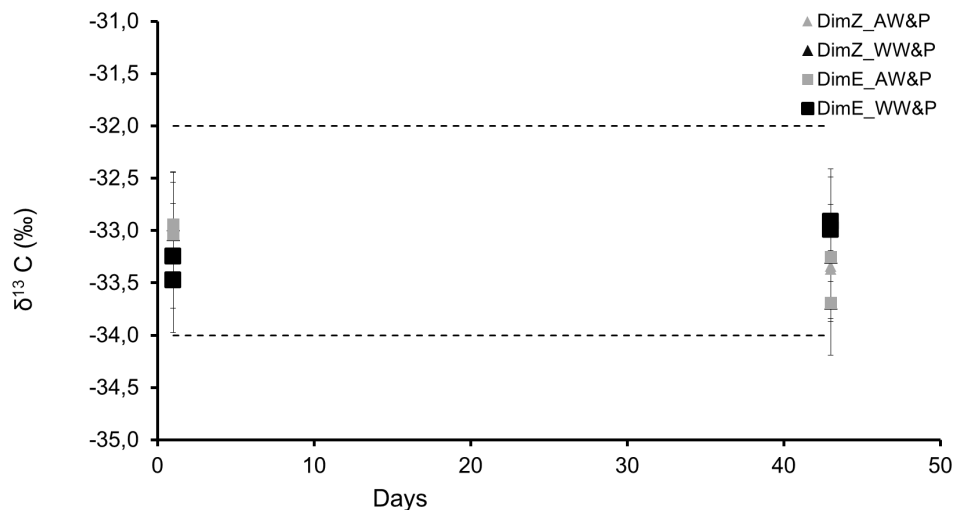
183



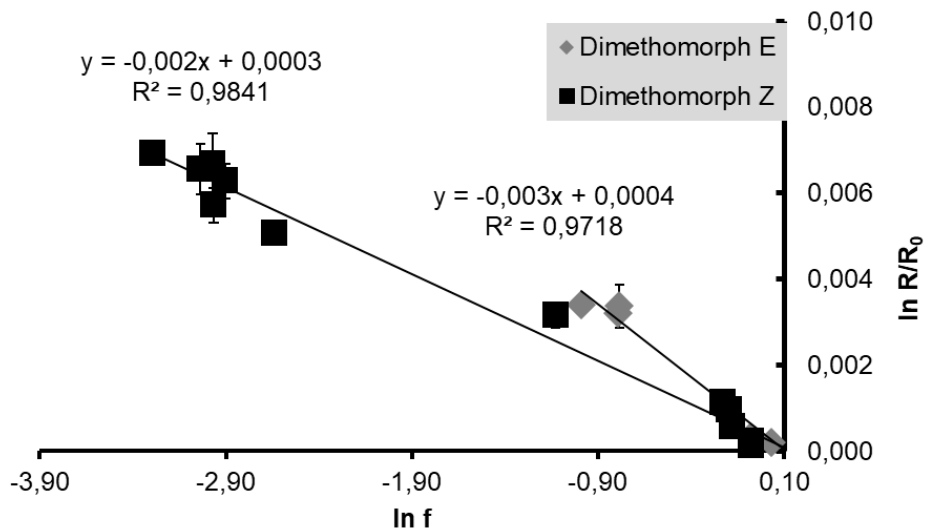
184

185 Figure S7. A- Fraction remaining of Z (triangles) and E (squares) isomers of DIM over time for  
186 plant activity was measured with autoclaved water (AW&P) microcosms (gray symbols) and plant

187 activity was measured with non-autoclaved water WW&P microcosms (black symbols); B- semi  
 188 dark (SD) controls (gray symbols) and dark (D) controls (black symbols).



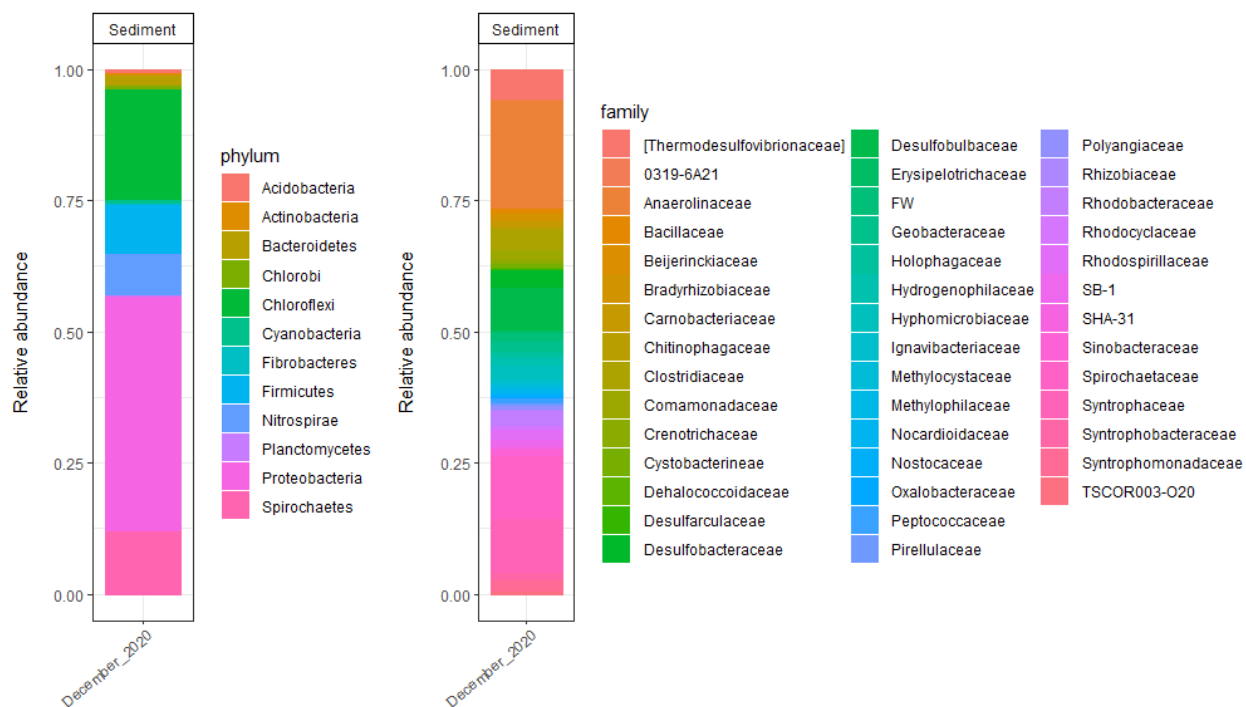
189  
 190  
 191 Figure S8. Carbon isotope signature ( $\delta^{13}C$ ) of Z (triangles) and E (squares) isomers of DIM  
 192 measured over time for plant activity with autoclaved water (AW&P) microcosms (gray symbols)  
 193 and plant activity with non-autoclaved water (WW&P) microcosms (black symbols).



194  
 19  
 19

195 Figure S9. Rayleigh plot for carbon isotopes for DIM Z and E: fraction of degradation during  
 196 sediment experiment ( $\ln f$ ) versus  $\ln R/R_0 = (\delta^{13}C+1000)/(\delta^{13}C_0+1000)$ .

197



198

199 Figure S10. Bacterial community composition of the sediment collected in Rouffach in December  
 200 2020 at phylum and family level.

201

202

203

204

205 **References**

- 206 Droz, B., Drouin, G., Maurer, L., Villette, C., Payraudeau, S. and Imfeld, G. 2021. Phase Transfer and  
207 Biodegradation of Pesticides in Water-Sediment Systems Explored by Compound-Specific Isotope  
208 Analysis and Conceptual Modeling. *Environ Sci Technol* 55(8), 4720-4728.
- 209 Gilevska, T., Masbou, J., Baumlin, B., Chaumet, B., Chaumont, C., Payraudeau, S., Tournebize, J., Probst,  
210 A., Probst, J.L. and Imfeld, G. 2022. Do pesticides degrade in surface water receiving runoff from  
211 agricultural catchments? Combining passive samplers (POCIS) and compound-specific isotope  
212 analysis. *Sci Total Environ* 842, 156735.
- 213 Gong, W., Jiang, M., Zhang, T., Zhang, W., Liang, G., Li, B., Hu, B. and Han, P. 2020. Uptake and  
214 dissipation of metalaxyl-M, fludioxonil, cyantraniliprole, and thiamethoxam in greenhouse  
215 chrysanthemum. *Environ Pollut* 257, 113499.
- 216 Grégoire, C., Payraudeau, S. and Domange, N. 2010. Use and fate of 17 pesticides applied on a vineyard  
217 catchment. *International Journal of Environmental and Analytical Chemistry* 90(3-6), 406-420.
- 218 Maillard, E. and Imfeld, G. 2014. Pesticide Mass Budget in a Stormwater Wetland. *Environ Sci Technol*  
219 48(15), 8603-8611.
- 220 Maillard, E., Payraudeau, S., Faivre, E., Gregoire, C., Gangloff, S. and Imfeld, G. 2011. Removal of  
221 pesticide mixtures in a stormwater wetland collecting runoff from a vineyard catchment. *Sci Total*  
222 *Environ* 409(11), 2317-2324.
- 223 Min, B.-M. 2015. Distribution properties of *Phragmites australis* and *Phacelurus latifolius* in the tidal-flat  
224 of Suncheon Bay. *Journal of Ecology and Environment* 38(1), 57-65.
- 225 Riedo, J., Wettstein, F.E., Rosch, A., Herzog, C., Banerjee, S., Buchi, L., Charles, R., Wachter, D., Martin-  
226 Laurent, F., Bucheli, T.D., Walder, F. and van der Heijden, M.G.A. 2021. Widespread Occurrence  
227 of Pesticides in Organically Managed Agricultural Soils-the Ghost of a Conventional Agricultural  
228 Past? *Environ Sci Technol* 55(5), 2919-2928.
- 229 Williams, A.J., Grulke, C.M., Edwards, J., McEachran, A.D., Mansouri, K., Baker, N.C., Patlewicz, G.,  
230 Shah, I., Wambaugh, J.F., Judson, R.S. and Richard, A.M. 2017. The CompTox Chemistry  
231 Dashboard: a community data resource for environmental chemistry. *J Cheminform* 9(1), 61.

232